https://doi.org/10.1016/j.apm.2017.10.035

On sparse beamformer design with reverberation

Zhibao Li, [1] Ka Fai Cedric Yiu*[2] and Yu-Hong Dai[3]

Abstract

Microphone array beamforming is one of the most important techniques to enhance the signal of interest from its observations corrupted by interference, noise and reverberation. In designing the beamformer to fulfill a desire performance, the transfer function governing sound propagation is required in the formulation. In general, the beamformer usually contains a number of FIR filters with long length behind each of microphone element, especially in reverberant environment. In order to reduce complexity, it is favourable to have many zero coefficients in the FIR filters. In this paper, we study this kind of sparse beamformer design problem. We first describe the transfer function developed for reverberant environment. Then we develop an L_2-L_p minimization model with $0 < p < 1$ for the design of sparse beamformers and introduce the smoothing Barzilai-Borwein (BB) step gradient method for solving the problem. Experimental results show that the designed beamformers achieve comparable performance with rather sparse filter coefficients.

Keywords:
Sparse beamformer design, Reverberation, Nonconvex optimization, Smoothing approximation, Smoothing BB-gradient method.

1. Introduction

Over the last few decades, the microphone array beamforming techniques have been extensively investigated and applied in teleconferencing, hands-free communication and speech acquisition [1, 2, 3, 4]. In general, there are two key factors that will determine the beamformer performance: the number of microphone elements and the length of the corresponding FIR filters. In order to achieve better performance on speech enhancement, one needs to increase the number of microphone elements and the length of the FIR filters, especially in reverberant environment.

It is noted that optimal beamforming arrays are usually achieved at non-uniformly configurations as indicated by the placement design problems [5, 6, 7, 8, 9, 10], and the increase of microphone elements is usually not as flexible as the filter length. Indeed, most studies on beamformer design have been focused on the optimization of the filter coefficients. For instance, a penalty function method has been developed to formulate the minimax near-field beamformer design problem as an unconstrained nonlinear optimization problem in [11]. Then, the minimax problem has been transformed into an equivalent problem by minimizing an auxiliary function in [12], and the solution has been given by the first root of this auxiliary function. In [13], the L_1-norm measure and the real rotation theorem have been used to formulate the problem as a semi-infinite linear programming problem. A least-squares indoor beamformer design problem has been developed based on L_2-norm in [14]. Some multi-criteria optimization models based on L_1-norm for the indoor beamformer design have been studied in [15, 16].

At the same time, it should be noted that the complexity of a beamformer system is dominated by arithmetic operations, and the number of nonzero filter coefficients is the major metric. The computational savings for a system will be realized by omitting arithmetic operations associated with those zero-valued coefficients. Moreover, it is found that many of the solved filter coefficients are close to zeros during the beamformer design, and the design of beamforming filters with relatively few nonzero coefficients providing near-optimal performance becomes meaningful as a technique for reducing complexity. A class of approximate polynomial-time algorithms by using the linear programming to design sparse filters have been proposed in [17]. The early optimization model for the sparse beamformer design was formulated as the basis pursuit problem in [17]; however, it was shown that the kind of problems as basis pursuit are NP-hard [18] and computationally difficult. Therefore, some heuristic techniques and approximate approaches were introduced for the sparse filter design, such as successive thinning and the L_1-norm approximation proposed in [17]. Moreover, some L_1/L_p-norm mixing models with $p > 1$ have been developed to induce the group sparsity of the beamformer coefficients in [19, 20], as well as the L_1/L_∞-norm for antenna selection [21]. The Tikhonov regularization has also been attempted in [22, 23].

As a matter of fact, using L_p minimization with $0 < p < 1$ can achieve better performance than basis pursuit or sparse reconstruction [24, 25, 26]. Chartrand and Yin proposed an iteratively reweighted algorithms to compute the local minima of such nonconvex problem in [27]. In addition, since the L_p-like minimization problem is nonsmooth and non-Lipshchitz, many smoothing approximation techniques have been developed trying to solve the L_p-like minimization problem numerically. For instance, the smoothing gradient method proposed by Chen in [28], smoothing quadratic regularization method proposed by Bian and Chen in [29], interior point algorithms proposed by Bian *et al.* in [30], more studies on the smoothing methods can be seen in the monographs [31, 32], and so on. There are also many recent studies on the complexity analysis of the L_p-like minimization problem with $0 < p < 1$, such as the lower bound theory of sparse solution for the L_2-L_p minimization problem in [33], complexity analysis in [34], and the complexity of unconstrained L_2-L_p minimization in [35], and so on.

In this paper, we propose a novel sparse beamformer design method in a reverberant environment. We first develop the transfer function to include the effect of reverberation. Based on that, we formulate the sparse beamformer design problem into an L_2-L_p minimization problem with $0 < p < 1$. Due to the fact that this L_2-L_p minimization problem is nonsmooth and non-Lipshchitz, we introduce the smoothing approximation technique to solve it numerically. In general, there are three steps for developing a smoothing method to solve a nonsmooth, nonconvex optimization problem: (i) define a smoothing function, many kinds of smoothing functions can be used to approximate the L_p-norm term in the sparse beamformer design model, see [36, 28, 29] and the reference therein; (ii) choose an algorithm to solve the approximated smoothing optimization problem, a variety of effective smoothing algorithms have been developed in recent[28, 29, 37]; (iii) update the smoothing parameter.

The rest of the paper is organized as follows. In Section II, we describe the signal model and formulate the beamformer design problem into a least squares problem. In Section III, we discuss the process of sound wave propagation and the image source method for estimating the room impulse responses. Then, we formulate an unconstrained L_2-L_p minimization model for the design of sparse beamformer, and introduce the smoothing Barzilai-Borwein (BB) step gradient method to solve it in Section IV. Numerical experiments have been conducted to evaluate the performance of the proposed sparse beamformer design method in Section V. A brief conclusion is given in the final Section VI.

2. Beamformer design modelling

In this section, we first describe the microphone array signal processing modelling and the simplest beamformer design problem. Under the measure of the L_1-norm, the beamformer coefficients are in fact required to satisfy a linear system in a given discrete space. Consider an N-element microphone array with L-tap FIR filter behind each of microphone in an acoustic environment, suppose the microphone elements have been set at a given placement $\{(x_i, y_i, z_i),\ i = 1, 2, \ldots, N\}$, then the beamformer design problem is to design a group of L-tap FIR filters $\boldsymbol{w} = [\boldsymbol{w}_1^T, \boldsymbol{w}_2^T, \ldots, \boldsymbol{w}_N^T]^T$, such that the objective of directional signal transmission or reception. If the signals received by the microphone array are sampled synchronously at the rate of f_s per second, therefore, the frequency responses of these FIR filters may be defined as

$$W_i(\boldsymbol{w}, f) = \boldsymbol{w}_i^T \boldsymbol{d}_0(f), \quad i = 1, 2, ..., N, \tag{1}$$

where $\boldsymbol{w}_i = [w_i(0), w_i(1), ..., w_i(L-1)]^T$ is a coefficient vector consisting of the i-th $L-$tap FIR filter, and $\boldsymbol{d}_0(f) = [1, \exp\{-j2\pi f/f_s\}, \ldots, \exp\{-j2\pi f(L-1)/f_s\}]^T$.

Denote the room impulse responses (RIRs) characterizing the sound wave propagation from the space point $\boldsymbol{r} = (x, y, z) \in \Omega$ to the i-th microphone element as $R_i(\boldsymbol{r}, f)$, which can be estimated by some room acoustic simulators. In particular, we apply the image source method [38, 39] which is described in Appendix. Then the beamforming target is to find a group of filter coefficients $\boldsymbol{w}$, such that the beamformer response

$$G(\boldsymbol{r}, f) = \sum_{i=1}^{N} W_i(\boldsymbol{w}, f) R_i(\boldsymbol{r}, f) = \boldsymbol{R}^T(\boldsymbol{r}, f)\boldsymbol{W}(\boldsymbol{w}, f), \tag{2}$$

is as close to a desired response $G_d(\boldsymbol{r}, f)$ from the space point $\boldsymbol{r}$ to the beamformer output point $\boldsymbol{r}_{\text{out}}$ as possible, where $\boldsymbol{R}(\boldsymbol{r}, f) = [R_1^T(\boldsymbol{r}, f), \ldots, R_N^T(\boldsymbol{r}, f)]^T$ is the frequency domain RIR vector, and $\boldsymbol{W}(\boldsymbol{w}, f) = [W_1^T(\boldsymbol{w}, f), \ldots, W_N^T(\boldsymbol{w}, f)]^T$ is the vector of frequency responses.

One simplest mathematic model for the beamformer design is to define a linear system as follows

$$\boldsymbol{R}^T(\boldsymbol{r}, f)\boldsymbol{W}(\boldsymbol{w}, f) - G_d(\boldsymbol{r}, f) = 0, \quad \text{for all} \quad (\boldsymbol{r}, f) \in \Omega, \tag{3}$$

where Ω is the space-frequency domain of interest. There are also many other optimization models have been developed from a framework of minimizing the maximum error between the beamformer response and desired response for the beamformer design based on the L_1-norm or L_2-norm in the literature [13, 14, 15]. Consider the formulated linear system (3), which is a semi-infinite problem because it is defined in a continuous space-frequency region Ω. In order to deal with the beamformer design problem numerically, the discretization methods and reduction based approaches [40, 41, 42, 43] are usually introduced to transform such semi-infinite problem (3) into some finite numerical problem approximately, and sequences of adaptive meshes can be applied so that the meshes are refined gradually.

Let a multi-dimensional grid region Ω_M be an approximation of the space-frequency domain Ω with a uniform grid containing M mesh points in each dimension. By merging the RIR vecotors $\boldsymbol{R}(\boldsymbol{r}, f)$ and vector $\boldsymbol{d}_0$ together into a new vector $\boldsymbol{d}(\boldsymbol{r}, f)$, we can rearrange the beamformer response as

$$\boldsymbol{R}^T(\boldsymbol{r}, f)\boldsymbol{W}(\boldsymbol{w}, f) = \boldsymbol{w}^T\boldsymbol{d}(\boldsymbol{r}, f). \tag{4}$$

If we expand the complex functions as

$$\boldsymbol{d}(\boldsymbol{r}, f) = \boldsymbol{d_1}(\boldsymbol{r}, f) + j\boldsymbol{d_2}(\boldsymbol{r}, f), \quad G_d(\boldsymbol{r}, f) = G_{d_1}(\boldsymbol{r}, f) + jG_{d_2}(\boldsymbol{r}, f),$$

where $\boldsymbol{d_1}(\boldsymbol{r}, f)$, $\boldsymbol{d_2}(\boldsymbol{r}, f)$, $G_{d_1}(\boldsymbol{r}, f)$ and $G_{d_2}(\boldsymbol{r}, f)$ are the real and imaginary parts of $\boldsymbol{d}(\boldsymbol{r}, f)$ and $G_d(\boldsymbol{r}, f)$, respectively. Thus, the beamformer design problem (3) can be divided into

$$\begin{cases} \boldsymbol{w}^T\boldsymbol{d_1}(\boldsymbol{r}, f) - G_{d_1}(\boldsymbol{r}, f) = 0, \\ \boldsymbol{w}^T\boldsymbol{d_2}(\boldsymbol{r}, f) - G_{d_2}(\boldsymbol{r}, f) = 0, \end{cases} \quad \text{for all} \quad (\boldsymbol{r}, f) \in \Omega_M. \tag{5}$$

In matrix formulation, the above beamformer design problem (5) will be rewritten as a standard linear equation problem like

$$\boldsymbol{A}\boldsymbol{w} - \boldsymbol{b} = \boldsymbol{0}, \tag{6}$$

where $\boldsymbol{A} = [\boldsymbol{d}_1(\boldsymbol{r}, f)\ \boldsymbol{d}_2(\boldsymbol{r}, f)\ \ \ldots]^T \in \mathbb{R}^{2M\times NL}$ is the composite matrix for all $(\boldsymbol{r}, f) \in \Omega_M$ and $\boldsymbol{b} = [G_{d_1}(\boldsymbol{r}, f)\ G_{d_2}(\boldsymbol{r}, f)\ \ \ldots]^T \in \mathbb{R}^{2M}$ is the corresponding composite vector, $\boldsymbol{0} \in \mathbb{R}^{2M}$ is a constant vector with all the entries are 0.

In general, the deviation between the original semi-infinite system and the discrete problem can be reduced by increasing the number of discretization points, this makes that the linear equation (6) is over-determined. In order to solve a least squares sense solution, the beamformer design problem (6) is usually transformed into the following least squares problem

$$\min_{\boldsymbol{w}\in\mathbb{R}^{NL}} H(\boldsymbol{w}) := \frac{1}{2}||\boldsymbol{A}\boldsymbol{w} - \boldsymbol{b}||_2^2. \tag{7}$$

Therefore, the optimal beamformer coefficients can be obtained by solving the above least squares problem (7), that is

$$\boldsymbol{w}^* = (\boldsymbol{A}^T\boldsymbol{A})^{-1}\boldsymbol{A}^T\boldsymbol{b}. \tag{8}$$

3. Smoothing BB-step gradient method for sparse beamformer design

In this section, we study the sparse beamformer design problem. We first formulate the sparse beamformer design problem as an L_2-L_p minimization problem, then, we introduce the smoothing approximation of the nonsmooth and nonconvex problem, and apply the smoothing BB-step gradient method to solve it accordingly.

3.1. L_2-L_p minimization problem

In the following, we use $n = NL$ to denote the number of total filter coefficients, and use $(\boldsymbol{w})_i$ to denote the i-th entry of $\boldsymbol{w}$ for the distinction between $\boldsymbol{w}_i$ defined in previous. Firstly, we propose a general framework of sparse beamformer design by using L_p-norm regularization, i.e.,

$$\min_{\boldsymbol{w}\in\mathbb{R}^{n}} f(\boldsymbol{w}) := H(\boldsymbol{w}) + \sum_{i=1}^{n} \varphi(|(\boldsymbol{w})_i|^p), \tag{9}$$

where $H(\cdot)$ is the L_2-norm objective function defined in (7), $0 < p < 1$, and $\varphi : [0, +\infty) \mapsto [0, +\infty)$ is a given penalty function satisfying the following assumption.

Assumption 1. *φ is continuously differentiable, nondecreasing, φ' is locally Lipschitz continuous, and there is a positive constant ϱ such that $\forall\ t \in (0, \infty)$,*

$$0 \le \varphi'(t) \le \varrho, \quad |\xi| \le \varrho, \quad \text{and} \quad |\xi|t \le \varrho, \quad \forall\ \xi \in \partial(\varphi'(t)),$$

where ∂ means the Clarke generalized gradient [44].

Remark 1. *To illustrate that the application of L_p-norm regularization in statistics and sparse reconstruction is not restricted by assumption (1), there are many widely used penalty functions φ summarized in [28, 29], and the references therein, for instance,*

1. *soft thresholding penalty function:* $\varphi_1(t) = \lambda t$;

2. *logistic penalty function:* $\varphi_2(t) = \lambda \log(1 + at)$;

3. *fraction penalty function:* $\varphi_3(t) = \lambda \frac{at}{1+at}$;

4. *hard thresholding penalty function:* $\varphi_4(t) = \lambda^2 - (\lambda - t)_+^2$;

5. *smoothly clipped absolute deviation (SCAD) penalty function:*

$$\varphi_5(t) = \lambda \int_0^t \min\left\{1, \frac{(a - s/\lambda)_+}{a - 1}\right\} ds;$$

6. *minimax concave penalty (MCP) function:*

$$\varphi_6(t) = \lambda \int_0^t \left(1 - \frac{s}{as}\right)_+ ds;$$

where a and λ are two positive parameters, especially $a > 2$ in the SCAD penalty function and $a > 1$ in the MCP function.

The L_p-norm penalization has the power to force some coefficients to zeros and distinguish from the non-zero ones. There are many results reported in the literature on the use of an L_p-norm penalty in pursuit of sparse solutions theoretically and numerically [24, 45, 46, 26, 33]. However, the defined objective function $f(\boldsymbol{w})$ in (9) is non-Lipschitzian when $0 < p < 1$, and many well-known optimization algorithms are not suitable for dealing with nonsmooth, nonconvex objective functions.

Smooth approximation methods are effective and efficient techniques for dealing with both the nonsmooth objective functions and nonsmooth constraints [47, 31, 48, 49, 32, 50, 51, 28, 29]. By using smoothing methods, the optimization problems only have continuously differentiable functions, and there are lots of theories and powerful solution methods for solving them [50]. It is guaranteed to find the local minimizer or stationary point of the original nonsmooth problem by updating the smoothing parameter. However, the efficiency of a smoothing method depends on the smooth approximation function, the solution method for the smooth optimization problem, and the updating scheme for the smoothing parameter.

3.2. Smoothing approximation

The definition of smoothing function was proposed in [28] as follows:

Definition 1. *Let $f : \mathbb{R}^n \mapsto \mathbb{R}$ be a continuous function. We call $\bar{f} : \mathbb{R}^n \mapsto \mathbb{R}$ a smoothing function of f , if $\bar{f}(\cdot, \mu)$ is continuously differentiable in $\mathbb{R}^n$ for any fixed $\mu > 0$, and for any $\boldsymbol{w} \in \mathbb{R}^n$,*

$$\lim_{\boldsymbol{v} \to \boldsymbol{w},\ \mu \downarrow 0} \bar{f}(\boldsymbol{v}, \mu) = f(\boldsymbol{w}).$$

Based on the above Definition 1, a class of nonsmooth functions can be defined accordingly [36, 31, 52]. For the L_2-L_p minimization problem (9) on sparse beamformer design, there is a smoothing function for the absolute value function $|\cdot|$ to construct a smoothing function proposed in [29]. Given $s \in \mathbb{R}$, $\mu > 0$ and $\boldsymbol{w} \in \mathbb{R}^n$, we first define

$$\kappa(s,\mu) = 8\varrho p \begin{cases} \left|\frac{s}{2}\right|, & \text{if } |s| > 2\mu, \\ \mu^{p-2}, & \text{if } |s| \leq 2\mu, \end{cases} \qquad \theta(s,\mu) = \begin{cases} |s|, & \text{if } |s| > \mu, \\ \frac{s^2}{2\mu} + \frac{\mu}{2}, & \text{if } |s| \leq \mu; \end{cases} \tag{10}$$

and

$$\bar{f}(\boldsymbol{w},\mu) = H(\boldsymbol{w}) + \sum_{i=1}^{n} \varphi(\theta^p((\boldsymbol{w})_i,\mu)), \tag{11}$$

$$\bar{g}(\boldsymbol{w},\mu) = [\bar{g}_1(\boldsymbol{w},\mu), \bar{g}_2(\boldsymbol{w},\mu), \ldots, \bar{g}_n(\boldsymbol{w},\mu)]^T := \nabla_{\boldsymbol{w}} \bar{f}(\boldsymbol{w},\mu). \tag{12}$$

From the above definition, we can see that the $\theta(s,\mu)$ defined in (10) is the smoothing function of absolute value function $|\cdot|$. The following lemma shows that the smoothing function $\theta(s,\mu)$ also satisfies some interesting properties [29].

Lemma 1. *If $\theta(s,\mu)$ is defined as that in (10), it satisfies:*

(i) $|\nabla_s \theta(s,\mu)| \leq 1$, $\forall s \in \mathbb{R}$, $\mu \in (0,+\infty)$*;*

(ii) $\frac{\mu}{2} \leq \theta(s,\mu) \leq \mu$, $\forall |s| \leq \mu$*;*

(iii) $0 \leq \theta^p(s,\mu) - |s|^p \leq \theta^p(0,\mu) = \left(\frac{\mu}{2}\right)^p$, $\forall s \in \mathbb{R}$, $\mu \in (0,+\infty)$, $p \in (0,1]$.

Due to the continuous differentiability of functions φ and θ, $\varphi(\theta^p((s,\mu))$ is a smoothing function of $\varphi(|(\boldsymbol{w})_i|^p)$ and $\bar{f}(\boldsymbol{w},\mu)$ is a smoothing function of $f(\boldsymbol{w})$. And from the condition of Assumption 1 and Lemma 1 (iii), we have

$$0 \leq \bar{f}(\boldsymbol{w},\mu) - f(\boldsymbol{w}) \leq n\varrho \left(\frac{\mu}{2}\right)^p, \quad \forall \boldsymbol{w} \in \mathbb{R}^n,\ \mu \in [0,+\infty).$$

Moreover, based on results from Lemma 1 and Rademacher's theorem, the smoothing function $\varphi(\theta^p((s,\mu))$ has the following property.

Proposition 1. *For any $\mu > 0$ and $s, \hat{s} \in \mathbb{R}$ such that $|s - \hat{s}| \leq \max\{\frac{\hat{s}}{2}, \mu\}$, the following inequality holds,*

$$\varphi(\theta^p((s,\mu)) \leq \varphi(\theta^p((\hat{s},\mu)) + \langle \nabla_{\hat{s}} \varphi(\theta^p((\hat{s},\mu)), s - \hat{s} \rangle + \frac{\kappa(\hat{s},\mu)}{2}(s-\hat{s})^2. \tag{13}$$

Proof. See the details in [29].

By using the smoothing function defined above, we obtain a smoothing approximation to the L_2-L_p minimization problem (9) as

$$\min_{\boldsymbol{w}\in\mathbb{R}^n} \bar{f}(\boldsymbol{w},\mu), \tag{14}$$

where $\bar{f}(\boldsymbol{w},\mu)$ is defined in (11). In order to solve the above smoothing approximation problem (14) for the sparse beamformer design, we introduce the smoothing BB-step gradient method in the next section.

3.3. Smoothing BB-step gradient (SBBG) algorithm

One customized numerical method for solving the kind of nonsmooth, nonconvex problem (9) is the class of smoothing gradient algorithms discussed in [28]. Gradient method using BB step converges R-superlinearly for two-dimensional strictly convex qudratic functions. However, traditional gradient method only converges linearly which is worse than the BB method. It has been observed in many numerical experiments that the BB method is preferable to other gradient methods. For example, [53, 54, 55, 56].

An efficient gradient-based smoothing method is the smoothing projected BB method for constrained non-Lipschitz optimization proposed by Huang and Liu [37]. They applied the projected gradient strategy to solve the smoothing approximation of constrained non-Lipschitz optimization problem by using the two BB-step sizes alternatingly. Here we adapt the method for solving the smoothing approximation of the unconstrained nonsmooth, nonconvex problem (14).

Consider the gradient iteration form

$$\boldsymbol{w}^{k+1} = \boldsymbol{w}^k - \alpha_k \boldsymbol{d}^k, \tag{15}$$

where α_k is the step size and $\boldsymbol{d}^k = -\bar{g}(\boldsymbol{w}^k,\mu_k)$ is the descent direction. At Barzilai and Borwein's suggestion [57], two choices of the step size α_k can improve the effectiveness of gradient methods significantly, they are

$$\alpha_k^{BB1} = \frac{\langle \boldsymbol{s}_{k-1}, \boldsymbol{s}_{k-1}\rangle}{\langle \boldsymbol{s}_{k-1}, \boldsymbol{y}_{k-1}\rangle}, \tag{16}$$

and

$$\alpha_k^{BB2} = \frac{\langle \boldsymbol{s}_{k-1}, \boldsymbol{y}_{k-1}\rangle}{\langle \boldsymbol{y}_{k-1}, \boldsymbol{y}_{k-1}\rangle}, \tag{17}$$

where $\boldsymbol{s}_{k-1} = \boldsymbol{w}^k - \boldsymbol{w}^{k-1}$ and $\boldsymbol{y}_{k-1} = \bar{g}(\boldsymbol{w}^k,\mu_k) - \bar{g}(\boldsymbol{w}^{k-1},\mu_{k-1})$. Moreover, the alternating use of the BB-step lengths (16) and (17) has been reported that it has better numerical performance [58, 59],

$$\alpha_k^{BB} = \begin{cases} \alpha_k^{BB1}, & \text{for odd } k; \\ \alpha_k^{BB2}, & \text{for even } k. \end{cases} \tag{18}$$

In the general non-quadratic case, introducing some nonmonotone line search scheme is necessary to guarantee the global convergence of the BB-step gradient method [53, 54, 60], as well as the requirements on the lower and upper bounds of the step length,

$$\alpha_k = \min\{\alpha_{\max}, \max\{\alpha_{\min}, \alpha_k^{BB}\}\}, \tag{19}$$

where $\alpha_{\max} > \alpha_{\min} > 0$. Therefore, we introduce the smoothing BB-step gradient algorithm for solving sparse beamformer design problem (9) as follows:

Algorithm 1. *(Smoothing BB-step gradient algorithm)*

Step 0: *Let* $\lambda > 0$, $0 < \sigma, \sigma_1, \sigma_2 < 1$, $\eta > 1$, $\alpha_{\max} > \alpha_{\min} > 0$, *choose an integer* $C \geq 1$, $\boldsymbol{w}^0 \in \mathbb{R}^n$, $\mu_0 > 0$, $\alpha_0 \geq 1$, *and set* $k = 0$.

Step 1: *Calculate the search direction with BB step size by*

$$\boldsymbol{d}^k = -\alpha_k \bar{g}(\boldsymbol{w}^k, \mu_k).$$

Choose the smallest nonnegative integer c_k *such that the steplength* $\lambda_k = \rho^{c_k}$ *satisfying*

$$\bar{f}(\boldsymbol{w}^k + \lambda_k \boldsymbol{d}^k, \mu_k) \leq \max_{0 \leq j \leq \min\{k, C-1\}} \bar{f}(\boldsymbol{w}^{k-j}, \mu_{k-j}) + \sigma \lambda_k \langle \bar{g}(\boldsymbol{w}^k, \mu_k), \boldsymbol{d}^k \rangle.$$

And set $\boldsymbol{w}^{k+1} = \boldsymbol{w}^k + \lambda_k \boldsymbol{d}^k$.

Step 2: *If* $\|\bar{g}(\boldsymbol{w}^{k+1}, \mu_k)\|_2 < \sigma_1 \mu_k$, *choose* $\mu_{k+1} = \sigma_2 \mu_k$; *otherwise, set* $\mu_{k+1} = \mu_k$.

Step 3: *If* $\langle \boldsymbol{w}_k, \boldsymbol{y}_k \rangle \leq 0$, *set* $\alpha_{k+1} = 1$; *otherwise, compute* α_{k+1} *by* (19).

Step 4: *Set* $k = k + 1$, *and return to Step 1.*

It is noted that global convergence of the Barzilai-Borwein gradient algorithm with non-monotone line search have been developed in[53]. Thus, the convergence results of the above Algorithm 1 can also be obtained.

4. Numerical experiments

In this section, we present a number of examples to illustrate the performance of the proposed smoothing BB-step gradient (SBBG) method on the design of sparse beamformers.

4.1. Microphone array system

For the first example, we choose a uniform linear array with 7-element microphones to setup in front of the target region in the space domain. The array spacing is setting as $0.06m$ that can avoid spatial aliasing for the frequency of interest, and an L-tap FIR filter is fixed behind each microphone element. In particular, we define the passband region as

$$\Omega_p = \{(\boldsymbol{r}, f) \mid x = 1m,\ |y-4| \le 0.4m,\ z = 1.5m,\ 0.5kHz \le f \le 2.0kHz\}, \tag{20}$$

and define the stopband regions as

$$\begin{aligned} \Omega_s = &\{(\boldsymbol{r}, f) \mid x = 1m,\ |y-4| \le 0.4m,\ z = 1.5m,\ 2.5kHz \le f \le 4.0kHz\}, \\ &\cup\{(\boldsymbol{r}, f) \mid x = 1m,\ 1.5m \le |y-4| \le 3.0m,\ z = 1.5m,\ 0.5kHz \le f \le 2.0kHz\}, \\ &\cup\{(\boldsymbol{r}, f) \mid x = 1m,\ 1.5m \le |y-4| \le 3.0m,\ z = 1.5m,\ 2.5kHz \le f \le 4.0kHz\}. \end{aligned} \tag{21}$$

For illustration, the diagram of the above microphone array system is depicted in Fig. 1.

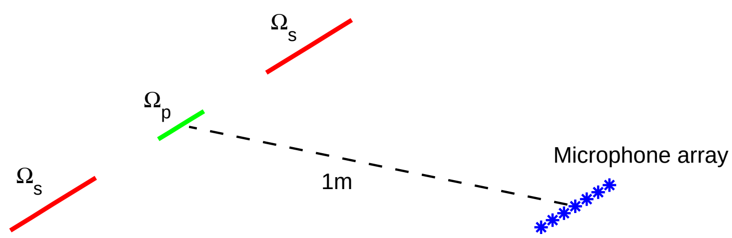

Figure 1: Layout of microphone array system for the free-field beamformer design.

In addition, the desired response function in the passband region Ω_p is given by

$$G_d(\boldsymbol{r}, f) = e^{-j2\pi f(\frac{||\boldsymbol{r}-\boldsymbol{r}_c||}{c} + \frac{L-1}{2f_s})},$$

where $\boldsymbol{r}_c$ is the center element of the microphone array, which is usually defined as the beamformer output point too, $f_s = 8000Hz$ is the sampling frequency. In the stopband region Ω_s, we simply define $G_d(\boldsymbol{r}, f) = 0$ to filter out the interference and noise. For the numerical modelling of beamformer design, we discrete the space-frequency domain of the passband Ω_p and stopband Ω_s into a grid of 30×30 frames, and use a more density grid scheme 120×120 to verify the beamforming performance.

4.2. Overall performance of the sparse beamformer

In the following, we choose the fixed filter length $L = 20$ to design different sparse beamformers and compare the performance with non-sparse beamformer. We use the soft thresholding penalty function $\varphi(t) = \lambda t$ to construct our sparse beamformer design model. For simplicity, the parameters in the proposed SBBG Algorithm 1 are set as

$$\sigma = \sigma_1 = \sigma_2 = 0.95,\ \eta = 2,\ \mu = 10,\ \beta_0 = 1,\ \ \alpha_{\max} = 10^8,\ \alpha_{\min} = 10^{-8},\ C = 5,\ \rho = 0.5.$$

From the construction of the $L_2 - L_p$ minimization model, we can see that the solution of problem (9) should be converged to the solution set of the least squares problem (7) as $\lambda \to 0$. In other words, the performance of the designed sparse beamformer should be close to the performance of the non-sparse beamformer when $\lambda \to 0$.

In order to verify the convergence, we firstly fix L_p-norm with $p = 0.5$, and choose different values for $\lambda = \{10^{-4},\ 10^{-3},\ 10^{-2},\ 10^{-1},\ 1,\ 10\}$ to design the sparse beamformers by using the proposed SBBG method. Then, we compare the performance of the designed sparse beamformers on the number of zeros, the passband gain, passband ripple and stopband ripple in Fig. 2. In the figures, we also plot the performance of the non-sparse beamformer derived from the LS model (7) for comparison. From the results shown in Fig. 2, we can see that: (i). the number of zeros (zero filter coefficients) in sparse beamformers designed by the SBBG method are increasing significantly with the growth of the the penalty parameter λ; moreover, there are fewer nonzeros in the sparse beamformers when λ less than 10^{-2}; (ii). the passband gains of the sparse beamformers are close to the non-sparse beamformer by LS method when λ is less than 10^{-1}, whereas they have poor performance when $\lambda > 1$; (iii). both the passband ripples and stopband ripples are close to the non-sparse beamformer when λ is less than 10^{-2}.

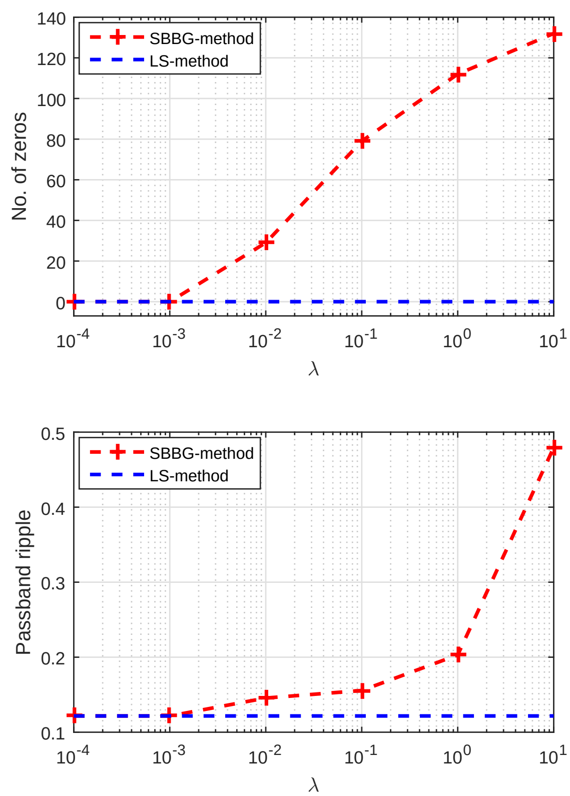

Figure 2: Comparison results on the performance of the sparse beamformer by using $L_2 - L_{0.5}$ minimization model v.s non-sparse beamformer by LS method.

We plot the overall performance and the filter coefficients of the non-sparse beamformer and sparse beamformers designed from the $L_2 - L_{0.5}$ minimization problem solved by the proposed

SBBG method in the following Fig. 3 and Fig. 4, respectively. From these figures, we can see that the sparse beamformer designed by the proposed SBBG method achieves comparable overall performance as the non-sparse beamformer for smaller λ, but with significant number of zero coefficients.

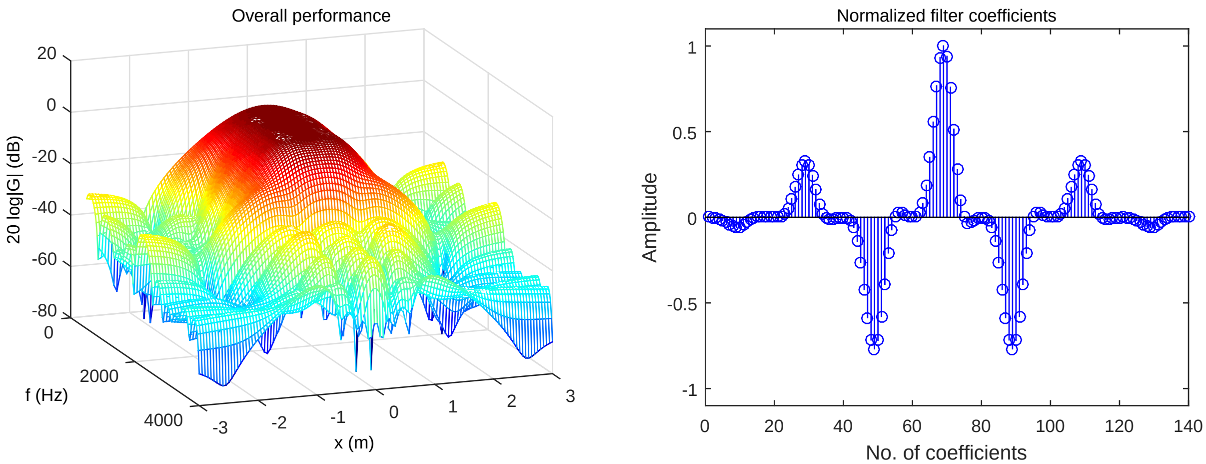

Figure 3: Overall performance of the beamformer designed from the LS-method.

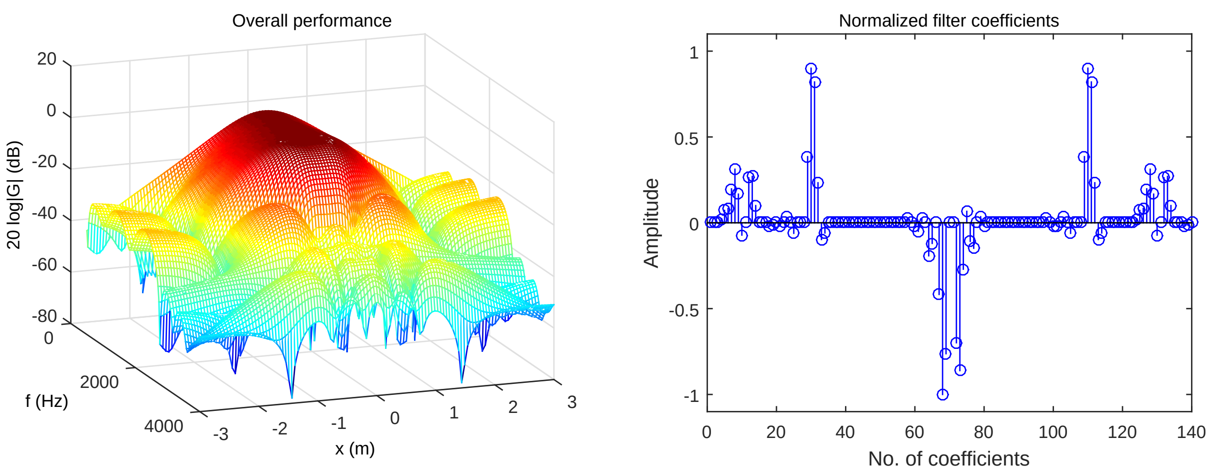

Figure 4: Overall performance of the sparse beamformer designed from the proposed SBBG method for solving the $L_2 - L_{0.5}$ minimization problem with $\lambda = 10^{-1}$.

4.3. Influence of the selection of L_p-norm

To study the influence of the selection of L_p-norm on the sparse beamformer design, we choose $p = \{0.1,\ 0.3,\ 0.5,\ 0.7,\ 0.9\}$ to formulated different $L_2 - L_p$ minimization models for the design of sparse beamformers as proposed in (9). Then, we apply the proposed SBBG method to solve them accordingly. The comparison results of the performance of the number of zeros in the sparse beamformers, the passband gain, the passband ripple and stopband ripple are plotted in Fig. 5.

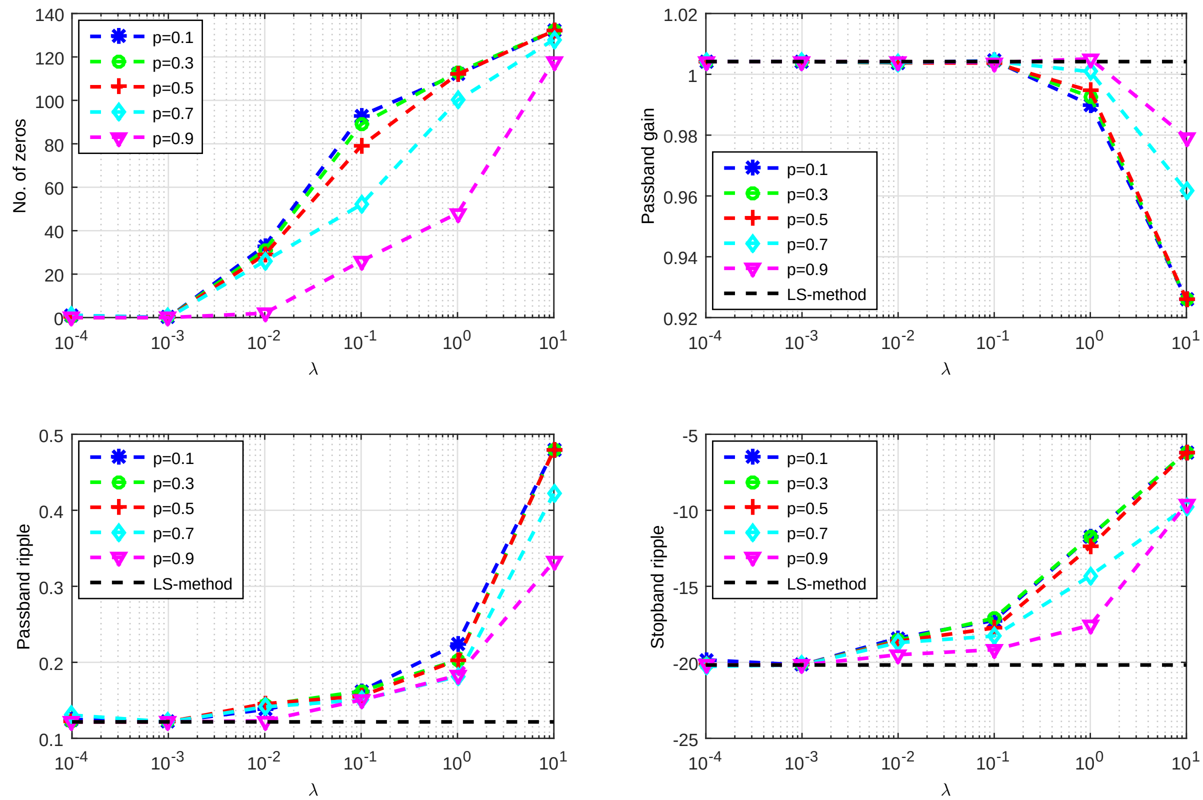

Figure 5: The comparison results of the sparse beamformers designed by using SBBG-method with different selection of L_p-norms.

From the results shown in Figure 5, we can conclude similarly that the number of zero coefficients increases as λ increasing for all $L_2 - L_p$ minimization models, and the performance is poorer for very large λ. Moreover, the selection of larger p in the sparse beamformer design will generate fewer number of zero coefficients, but the designed sparse beamformer has better performance on the passband gain, passband ripple and stopband ripple.

4.4. Indoor sparse beamformer design

In this subsection, we apply the proposed SBBG method to the sparse beamformer design in a reverberant environment. A simple rectangular room with 4m×8m×3m is constructed and the reverberation time $T_{60} = 0.1$s is tested. We introduce the fast-ISM room simulator by Lehmann and Johansson in [39] to estimate the room impulse responses, and setup a uniform linear array with 7-element microphones in front of the target region in the space domain (see the depiction in Fig. 6). We define the passband and stopband regions as the same as with the definitions in (20) and (21), and use a 20-tap FIR filter behind each microphone element.

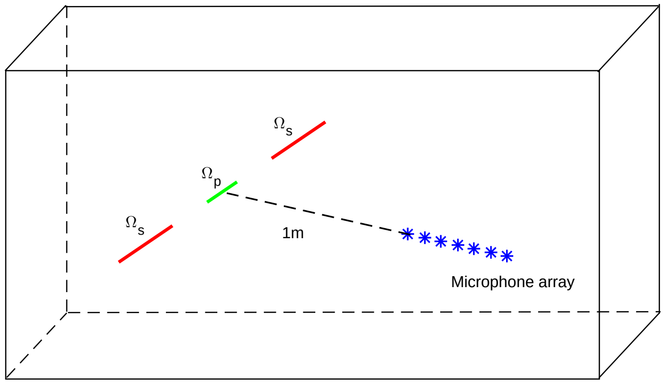

Figure 6: Layout of microphone array system for the indoor beamformer design.

We apply the $L_2 - L_{0.5}$ minimization model for the sparse beamformer design by the SBBG method in the indoor system. The overall performance and the filter coefficients of the non-sparse beamformer and sparse beamformers designed by the SBBG method with reverberation time $T_{60} = 0.1s$ are plotted in Fig. 7 and Fig. 8. From these figures, we can see that the sparse beamformers can achieve comparable performance as the non-sparse beamformers with much fewer nonzero coefficients.

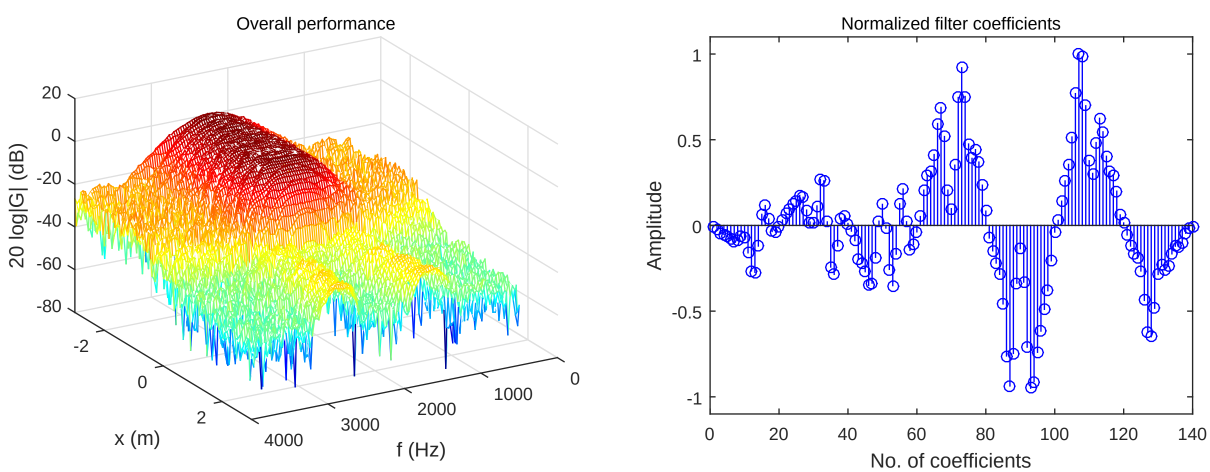

Figure 7: Overall performance of the indoor beamformer designed from the LS-method at $T_{60} = 0.1$s.

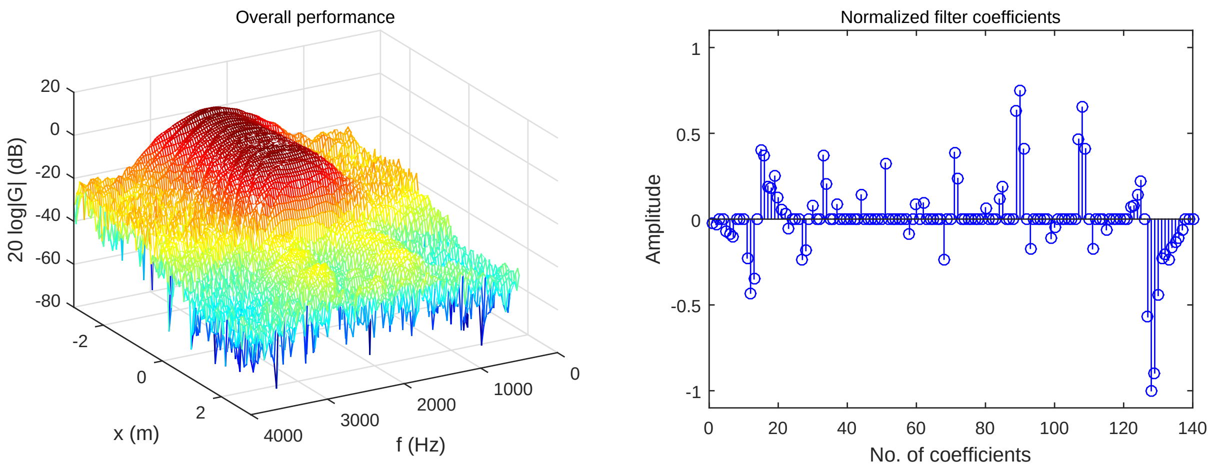

Figure 8: Overall performance of the indoor sparse beamformer designed from the proposed SBBG method for solving the $L_2 - L_{0.5}$ minimization problem with $\lambda = 10^{-1}$ at $T_{60} = 0.1$s.

5. Conclusion

In this paper, we have formulated the sparse beamformer design problem in a reverberant environment. Due to the nonsmooth and nonconvex difficulty, we introduced the smoothing approximation technique and developed the smoothing BB-step gradient method for finding good beamformer designs. We also conduct numerical experiments to verify the effectiveness of the proposed smoothing BB-step gradient method. Simulation results have shown that the proposed smoothing BB-step gradient method can design very good sparse beamformers for both indoor and outdoor applications.

Acknowledgements

The first author is supported by the Chinese Natural Science Foundation (No. 11701575), the second author is supported by GRF Grant PolyU. 152200/14E and PolyU Grant 4-ZZGS, the third author is supported by the Chinese Natural Science Foundation (Nos. 11631013, 71331001, 11331012) and the National 973 Program of China (No. 2015CB856002). Moreover, the authors would like to thank Dr. Yakui Huang for the interesting discussions on this paper.

Appendix

In this section, we briefly describe the acoustic transfer function for sound wave propagation and the image source method for the estimation of RIRs. In principle, the acoustic field can be viewed as a mixture of numerous simple plane waves, and their propagations are governed by the Euler's equation (Newton's 2^{nd} law applied to fluid) [61]. For a homogeneous medium undergoing inviscid fluid flow with a point source $s(\boldsymbol{r}, t)$, the wave equation can be written as

$$\nabla^2 p(\boldsymbol{r}, t) - \frac{1}{c^2}\frac{\partial^2 p(\boldsymbol{r}, t)}{\partial t^2} = -s(\boldsymbol{r}, t), \tag{22}$$

where $\nabla^2 = \frac{\partial^2}{\partial x^2} + \frac{\partial^2}{\partial y^2} + \frac{\partial^2}{\partial z^2}$ is the *Laplacian* operator in the Cartesian coordinates (x, y, z), c is the speed of sound, and $p(\boldsymbol{r}, t)$ is used to denote the sound pressure of position $\boldsymbol{r}$ at time t.

Applying the Fourier transform to the wave equation (22) as

$$P(\boldsymbol{r}, f) \triangleq \mathcal{F}\{p(\boldsymbol{r}, t)\}(f) = \int_{-\infty}^{\infty} p(\boldsymbol{r}, t) e^{j2\pi f t} dt, \tag{23}$$

we will get the time-independent Helmholtz equation as

$$\nabla^2 P(\boldsymbol{r}, f) + \kappa^2 P(\boldsymbol{r}, f) = -S(\boldsymbol{r}, f), \tag{24}$$

where $S(\boldsymbol{r}, f)$ is the Fourier transform of source $s(\boldsymbol{r}, t)$, and κ is the wave number related to the angular frequency $2\pi f$ and wave length ϱ through

$$\kappa = \frac{2\pi f}{c} = \frac{2\pi}{\varrho}.$$

Given a unit-amplitude harmonic point source at position $\boldsymbol{r}_s = [x_s, y_s, z_s]$, the source function in frequency domain is $S(\boldsymbol{r}, f) = \delta(\boldsymbol{r} - \boldsymbol{r}_s) = \delta(x - x_s)\delta(y - y_s)\delta(z - z_s)$, where $\delta(\cdot)$ denotes the Kronecker delta function. Then the partial differential equation (24) can be solved by first solving the inhomogeneous equation as

$$\Delta\mathcal{H}(\boldsymbol{r}, \boldsymbol{r}_s, f) + \kappa^2 \mathcal{H}(\boldsymbol{r}, \boldsymbol{r}_s, f) = \delta(\boldsymbol{r} - \boldsymbol{r}_s),$$

where $H(\boldsymbol{r}, \boldsymbol{r}_s, f)$ is the Green's function, or called the transfer function. Specially, in the free field, the Green's function related to the ominidirectional point source $\boldsymbol{r}_s$ is

$$\mathcal{H}(\boldsymbol{r}, \boldsymbol{r}_s, f) = \frac{1}{\|\boldsymbol{r} - \boldsymbol{r}_s\|} e^{\frac{-j2\pi f \|\boldsymbol{r} - \boldsymbol{r}_s\|}{c}}. \tag{25}$$

The transfer function (25) is widely used in the field of acoustic signal processing. But in the reverberant environment, such as office room, the propagation of sound wave will be changed by the reflections of walls, ceiling and floor, and the ideal transfer function model (25) is no longer effective to model the progression of sound wave propagation. There are approaches investigated for the room acoustic simulation, and the estimation of RIRs. Among them, the image source method (ISM) firstly proposed by Allen and Berkley in 1979 [38] is a popular technique for estimating the RIRs. A faster version of the ISM simulator was developed by Lehmann and Johansson in 2010 [39], where the estimation of reverberation tail have been modelled as decaying random noise to accelerate the process of simulation.

For a rectangular room with dimensions $\boldsymbol{L} = [L_x, L_y, L_z]^T$ containing a sound source and a microphone receiver, the ISM technique for measuring the RIR is to use the image source on an infinite grid of mirror rooms. The contribution of each image source to the captured signal is a replica of the source signal delayed by a lag τ and attenuated by an amplitude factor A. In general, the RIR from $\boldsymbol{r}_s$ to $\boldsymbol{r}_m$ is modelled as

$$h(t) = \sum_{\boldsymbol{\mu}=0}^{1} \sum_{\boldsymbol{\nu}=-\infty}^{+\infty} A(\boldsymbol{\mu}, \boldsymbol{\nu}) \cdot \delta(t - \tau(\boldsymbol{\mu}, \boldsymbol{\nu})), \tag{26}$$

where $\boldsymbol{\mu} = (\mu_x, \mu_y, \mu_z)^T$ and $\boldsymbol{\nu} = (\nu_x, \nu_y, \nu_z)^T$ are the image sources, $\boldsymbol{\beta} = \{\beta_{x,i}, \beta_{y,i}, \beta_{z,i}, i = 1, 2\}$ are the reflection coefficients for boundary of the room, and $A(\cdot)$ is the amplitude factor defined as

$$A(\boldsymbol{\mu}, \boldsymbol{\nu}) = \frac{\beta_{x,1}^{|x_m - x_s|} \beta_{x,2}^{|x_m|} \beta_{y,1}^{|y_m - y_s|} \beta_{y,2}^{|y_m|} \beta_{z,1}^{|z_m - z_s|} \beta_{z,2}^{|z_m|}}{4\pi d(\boldsymbol{\mu}, \boldsymbol{\nu})},$$

where $\tau(\boldsymbol{\mu}, \boldsymbol{\nu}) = d(\boldsymbol{\mu}, \boldsymbol{\nu})/c$ is the time delay of the considered image source, and $d(\cdot)$ represents the distance between $\boldsymbol{\mu}$ to $\boldsymbol{\nu}$. An illustration of the RIR estimated by the fast-ISM simulator is depicted in Fig. 9.

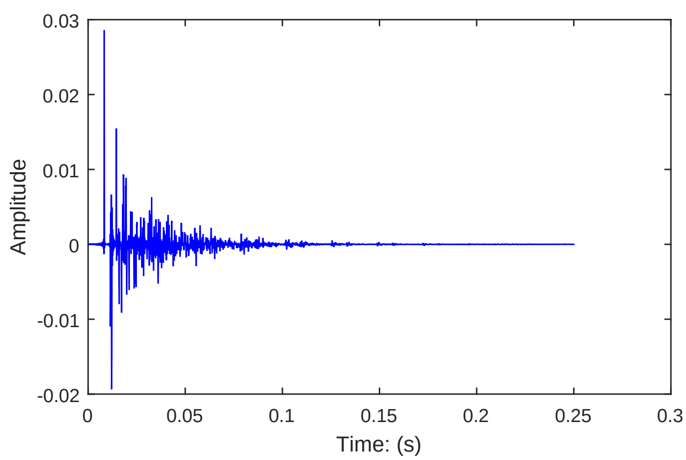

Figure 9: Illustration of RIR by ISM simulator.

References

[1] G. W. Elko, Microphone array systems for hands-free telecommunication, Speech Commun. 20 (3-4) (1996) 229–240.

[2] S. Fischer, K. U. Simmer, Beamforming microphone arrays for speech acquisition in noisy environments, Speech Commun. 20 (3-4) (1996) 215–227.

[3] M. Brandstein, D. Ward, Microphone Arrays: Signal Processing Techniques and Applications, Springer Verlag, Berlin, 2001.

[4] J. Benesty, J. Chen, Y. Huang, Microphone Array Signal Processing, Springer Verlag, Berlin, 2008.

[5] K. S. Chen, X. H. Yun, Z. S. He, C. L. Han, Synthesis of sparse planar arrays using modified real genetic algorithm, IEEE Trans. Antennas Propag. 55 (4) (2007) 1067–1073.

[6] G. Oliveri, A. Massa, Bayesian compressive sampling for pattern synthesis with maximally sparse non-uniform linear arrays, IEEE Trans. Antennas Propag. 59 (2) (2011) 467–481.

[7] D. Ayllón, R. Gil-Pita, M. Utrilla-Manso, M. Rose-Zurere, An evolutionary algorithm to optimize the microphone array configuration for speech acquisition in vehicles, Eng. Appl. Artif. Intel. 34 (2) (2014) 37–44.

[8] Z. G. Feng, K. F. C. Yiu, S. Nordholm, Placement design of microphone arrays in near-field broadband beamformers, IEEE Trans. Signal Process. 60 (3) (2012) 1195–1204.

[9] Z. B. Li, K. F. C. Yiu, Z. G. Feng, A hybrid descent method with genetic algorithm for microphone array placement design, Appl. Soft Comput. 13 (3) (2013) 1486–1490.

[10] Z. B. Li, K. F. C. Yiu, Beamformer configuration design in reverberant environments, Eng. Appl. Artif. Intel. 47 (2016) 81–87.

[11] S. Nordholm, V. Rehbock, K. L. Teo, S. Nordebo, Chebyshev optimization for the design of broadband beamformers in the near field, IEEE Trans. Circuits Syst. II 45 (1) (1998) 141–143.

[12] B. Lau, Y. Leung, K. Teo, V. Sreeram, Minimax filters for microphone arrays, IEEE Trans. Circuits Syst. II 46 (12) (1999) 1522–1525.

[13] K. F. C. Yiu, X. Q. Yang, S. Nordholm, K. L. Teo, Near-field broadband beamformer design via multidimensional semi-infinite linear programming techniques, IEEE Trans. Speech Audio Process. 11 (6) (2003) 725–732.

[14] Z. B. Li, K. F. C. Yiu, A least-squares indoor beamformer design, Pac. J. Optim. 9 (4) (2013) 697–707.

[15] Z. B. Li, K. F. C. Yiu, S. Nordholm, On the indoor beamformer design with reverberation, IEEE Trans. Audio, Speech, Language Process. 22 (8) (2014) 1225–1235.

[16] Z. B. Li, K. F. C. Yiu, Y. H. Chan, R. C. Leung, A novel indoor beamformer design method with obstacles, Pac. J. Optim. 12 (2) (2016) 233–243.

[17] T. Baran, D. Wei, A. V. Oppenheim, Linear programming algorithms for sparse filter design, IEEE Trans. Signal. Process. 58 (3) (2010) 1605–1617.

[18] S. Foucart, H. Rauhut, A mathematical introduction to compressive sensing, Basel: Birkhäuser, 2013.

[19] M. Hong, R. Sun, H. Baligh, Z. Q. Luo, Joint base station clustering and beamformer design for partial coordinated transmission in heterogeneous networks, IEEE J. Sel. Areas Commun. 31 (2) (2013) 226–240.

[20] J. Zhao, T. Q. Quek, Z. Lei, Coordinated multipoint transmission with limited backhaul data transfer, IEEE Trans. Wireless Commun. 12 (6) (2013) 2762–2775.

[21] O. Mehanna, N. Sidiropoulos, G. Giannakis, Joint multicast beamforming and antenna selection, IEEE Trans. Signal Process. 61 (10) (2013) 2660–2674.

[22] B. Li, H. H. Dam, A. Cantoni, K. L. Teo, A first-order optimal zero-forcing beamformer design for multiuser mimo systems via a regularized dual accelerated gradient method, IEEE Commun. Lett. 19 (2) (2015) 195–198.

[23] B. Li, C. Z. Wu, H. H. Dam, A. Cantoni, K. L. Teo, A parallel low complexity zero-forcing beamformer design for multiuser mimo systems via a regularized dual decomposition method, IEEE Trans. Signal Process. 63 (16) (2015) 4179–4190.

[24] J. Fan, R. Li, Variable selection via nonconcave penalized likelihood and its oracle properties, J. Amer. Statist. Assoc. 96 (456) (2001) 1348–1360.

[25] R. Chartrand, Exact reconstruction of sparse signals via nonconvex minimization, IEEE Signal Process. Lett. 14 (10) (2007) 707–710.

[26] J. Huang, J. L. Horowitz, S. Ma, Asymptotic properties of bridge estimators in sparse high-dimensional regression models, Ann. Statist. 36 (4) (2008) 587–613.

[27] R. Chartrand, W. Yin, Iteratively reweighted algorithms for compressive sensing, in: Proc. IEEE international conference on Acoustics, speech and signal processing, 2008, pp. 3869–3872.

[28] X. Chen, Smoothing methods for nonsmooth, nonconvex minimization, Math. Program. 134 (1) (2012) 71–99.

[29] W. Bian, X. Chen, Worst-case complexity of smoothing quadratic regularization methods for non-Lipschitz optimization, SIAM J. Optimiz. 23 (3) (2013) 1718–1741.

[30] W. Bian, X. Chen, Y. Ye, Complexity analysis of interior point algorithms for non-Lipschitz and nonconvex minimization, Math. Program. 149 (1-2) (2015) 301–327.

[31] R. T. Rockafellar, R. J. B. Wets, Variational Analysis, Springer, Berlin, 1998.

[32] Y. Nesterov, Smooth minimization of non-smooth functions, Math. Program. 103 (1) (2005) 127–152.

[33] X. Chen, F. Xu, Y. Ye, Lower bound theory of nonzero entries in solutions of l_2-l_p minimization, SIAM J. Sci. Comput. 32 (5) (2010) 2832–2852.

[34] D. Ge, X. Jiang, Y. Y. Ye, A note on the complexity of l_p minimization, Math. Program. 129 (2) (2011) 285–299.

[35] X. Chen, D. Ge, Z. Wang, Y. Ye, Complexity of unconstrained $l_2 - l_p$ minimization, Math. Program. 143 (1-2) (2014) 371–383.

[36] C. Chen, O. L. Mangasarian, A class of smoothing functions for nonlinear and mixed complementarity problems, Comput. Optim. Appl. 5 (2) (1996) 97–138.

[37] Y. K. Huang, H. W. Liu, Smoothing projected Barzilai-Borwein method for constrained non-Lipschitz optimization, Comput. Optim. Appl. 65 (3) (2016) 671–698.

[38] J. Allen, D. Berkley, Image method for efficiently simulating small-room acoustics, J. Acoust. Soc. Amer. 65 (4) (1979) 943–950.

[39] E. A. Lehmann, A. M. Johansson, Diffuse reverberation model for efficient image-source simulation of room impulse responses, IEEE Trans. Audio, Speech, Language Process. 18 (2010) 1429–1439.

[40] R. Fletcher, Practical Methods of Optimization, New York: Wiley, 1987.

[41] R. Hettich, K. Kortanek, Semi-infinite programming: Theory, methods, and applications, SIAM Rev. 35 (3) (1993) 380–429.

[42] R. Reemsten, S. Górner, Numerical methods for semi-infinite programming: A survey, Kluwer Academic, Boston, 1998.

[43] K. L. Teo, X. Q. Yang, L. S. Jennings, Computational discretization algorithms for functional inequality constrained optimization, Ann. Oper. Res. 98 (1-4) (2000) 215–234.

[44] F. H. Clarke, Optimization and Nonsmooth Analysis, John Wiley, New York, 1983.

[45] E. Candes, T. Tao, Decoding by linear programming, IEEE Trans. Inform. Theory 51 (12) (2005) 4203–4215.

[46] R. Chartrand, V. Staneva, Restricted isometry properties and nonconvex compressive sensing, Inverse Probl. 24 (3) (2008) 1–14.

[47] X. Chen, L. Qi, A parameterized Newton method and a quasi-Newton method for nonsmooth equations, Comput. Optim. Appl. 3 (2) (1994) 157–179.

[48] F. Facchinei, H. Jiang, L. Qi, A smoothing method for mathematical programs with equilibrium constraints, Math. Program. 85 (1) (1999) 107–134.

[49] M. Fukushima, Z. Q. Luo, P. Tseng, Smoothing functions for second-order-cone complementarity problems, SIAM J. Optim. 12 (2) (2002) 436–460.

[50] J. Nocedal, S. J. Wright, Numerical Optimization, 2nd Ed., Springer, New York, 2006.

[51] W. Bian, X. Chen, Smoothing neural network for constrained non-Lipschitz optimization with applications, IEEE Trans. Neural Netw. Learning Syst. 23 (3) (2012) 399–411.

[52] L. Qi, C. Ling, X. Tong, G. Zhou, A smoothing projected Newton-type algorithm for semi-infinite programming, Comput. Optim. Appl. 42 (1) (2009) 1–30.

[53] M. Raydan, The Barzilai and Borwein gradient method for the large scale unconstrained minimization problem, SIAM J. Optim. 7 (1) (1997) 26–33.

[54] E. G. Birgin, J. M. Martínez, M. Raydan, Nonmonotone spectral projected gradient methods on convex sets, SIAM J. Optim. 10 (4) (2000) 1196–1211.

[55] M. A. Figueiredo, R. D. Nowak, S. J. Wright, Gradient projection for sparse reconstruction: Application to compressed sensing and other inverse problems, IEEE J. Sel. Top. Signal Process. 1 (4) (2007) 586–597.

[56] S. J. Wright, R. D. Nowak, M. A. Figueiredo, Sparse reconstruction by separable approximation, IEEE Signal Process. Lett. 57 (7) (2009) 2479–2493.

[57] J. Barzilai, J. M. Borwein, Two-point step size gradient methods, IMA J. Numer. Anal. 8 (1) (1988) 141–148.

[58] L. Grippo, M. Sciandrone, Nonmonotone globalization techniques for the Barzilai-Borwein gradient method, Comp. Optim. Appl. 23 (2) (2002) 143–169.

[59] Y. H. Dai, J. Y. Yuan, Y. X. Yuan, Modified two-point stepsize gradient methods for unconstrained optimization, Comp. Optim. Appl. 22 (1) (2002) 103–109.

[60] Y. H. Dai, R. Fletcher, Projected Barzilai-Borwein methods for large-scale boxconstrained quadratic programming, Numer. Math. 100 (1) (2005) 21–47.

[61] H. Kuttruff, Room Acoustics, 4th ed, London: Spon Press, 2000.